

# Optimizing Antenna Activation for Even Power Distribution in Multi-Beam Satellite Systems Using Genetic Algorithm

Juan Andrés Vásquez-Peralvo, Aral Ertug Zorkun, Jorge Querol, Eva Lagunas, Flor Ortiz,  
Luis Manuel Garcés-Socarrás, Jorge Luis González-Rios, Symeon Chatzinotas.

Interdisciplinary Centre for Security Reliability and Trust, University of Luxembourg, 1855 Luxembourg-Luxembourg  
(e-mails: { juan.vasquez, aral.zorkun, jorge.querol, eva.lagunas, flor.ortiz, luis.garces,  
jorge.gonzalez, victor.monzon, symeon.chatzinotas}@uni.lu).

**Abstract**—Recent advancements in onboard satellite communication have significantly enhanced the ability to dynamically modify the radiation pattern of a Direct Radiating Array (DRA), which is essential for both conventional communication satellites like Geostationary Orbit (GEO) and those in lower orbits such as Low Earth Orbit (LEO). This is particularly relevant for communication at 28 GHz, a key frequency in the mmWave spectrum, used for high-bandwidth satellite links and 5G communications. Critical design factors include the number of beams, beamwidth, and Side Lobe Level (SLL) for each beam. However, in multibeam scenarios, balancing these design factors can result in uneven power distribution, leading to over-saturation in centrally located antenna elements due to frequent activations. This paper introduces a Genetic Algorithm (GA)-based approach to optimize beamforming coefficients by modulating the amplitude component of the weight matrix, while imposing a constraint on activation instances per element to avoid over-saturation in the Radio Frequency (RF) chain. The proposed method, tested on an  $16 \times 16$  DRA patch antenna array at 28 GHz for a CubeSat orbiting at 500 km, demonstrates how the algorithm efficiently meets beam pattern requirements and ensures uniform activation distribution. These findings are particularly relevant for emerging satellite systems and 5G networks operating in the mmWave spectrum.

**Index Terms**—array thinning, beamforming, beam synthesis, genetic algorithm, satellite communication.

## I. INTRODUCTION

Digital beamforming is becoming easier to get and use, which is making phased arrays even more popular [1]. Since there is a trade-off between signal processing and hardware, new applications are emerging where the phased antenna arrays are in need [2]. However, cost and power consumption push the digital beamforming into the background [3] where each antenna element requires active RF components [4]. Therefore, power optimization is crucial, especially in satellite systems, where flexible payloads are the most important [5].

In the context of flexible beamforming within a phased array system, achieving the desired beam characteristics — such as adjustable beam shape, SLL, and null steering is essential for adaptability. Deterministic beamforming techniques, such as Fast Fourier Transform (FFT), Zero Forcing (ZF),

and Singular Value Decomposition (SVD), can be employed to steer beams in specific directions while creating nulls in others. SLL control can be achieved through amplitude tapering, where the power distribution across antenna elements is varied [6]. However, these methods are not sufficient for generating complex beam shapes nor suitable for applying amplitude control to achieve specific beamwidths or sidelobe levels where power efficiency and heat dissipation are critical (multibeam scenarios) [7]. Another approach is the use of artificial intelligence to determine the required weight vector to address required beam characteristics with an approach of optimized power consumption [8], but this approach requires a data set that must be obtained using any other technique.

To address these challenges, this paper proposes a solution for generating beams with flexible beamwidth, and SLL by implementing array thinning to avoid reliance on amplitude tapering. By reducing the number of active elements in a controlled manner, array thinning helps maintain power efficiency while achieving the desired beam characteristics. Additionally, we introduce a constraint to distribute power more evenly across antenna elements by limiting their activation instances. In a typical scenario, generating multiple beams would require each antenna element to deliver power for all beams simultaneously, resulting in excessive power demands. In contrast, our proposed approach limits the number of antenna activation per beam. Once the maximum activation limit is reached for a given element, the algorithm dynamically selects a free element to take over, ensuring an even distribution of power and reducing thermal stress across the array.

## II. RADIATION PATTERN PARAMETERS

This section describes the antenna that will be used, its parameters that will be considered in the optimization algorithm.

### A. Unit Cell

The antenna used in this analysis is an open-ended waveguide since we are targeting low losses and high directivity. The radiation pattern of the open-ended waveguide can be modeled using the following electric field  $\mathbf{E}(r, \theta, \phi)$  formula:

$$\hat{\mathbf{E}}(r, \theta, \phi) = E_0 \frac{J_1(ka \sin \theta)}{ka \sin \theta} \frac{e^{-jkr}}{r} \left( \cos(\phi) \hat{\theta} + j \sin(\phi) \hat{\phi} \right) \quad (1)$$

where:

- $E_0$  is the amplitude scaling factor.
- $J_1$  represents the Bessel function of the first kind of order 1.
- $k = \frac{2\pi}{\lambda}$  is the wave number.
- $a$  denotes the radius of the waveguide.
- $r$  indicates the distance from the waveguide's aperture.
- $\theta$  and  $\phi$  are the polar and azimuthal angles, respectively.
- $\hat{\theta}$  and  $\hat{\phi}$  are unit vectors in the polar and azimuthal directions.

For easiness of computation and understanding of results, we compute the normalized power pattern as [9]:

$$\mathbf{U}(\theta, \phi) = \frac{|E(\theta, \phi)|^2}{\max(|E(\theta, \phi)|^2)}$$

In this paper we select an antenna aperture of  $0.58 \lambda$  ( $a = 0.3\lambda$ ) and an inter element space between antennas of  $0.6\lambda$ .

### B. Antenna Parameters

The parameters included in the optimization process are: beamwidth and SLL. Following, we will describe each of them and how can be extracted from the calculated radiation pattern.

1) *Beamwidth*: The average value obtained from different radiation pattern cuts is used to determine the beamwidth of each beam in the radiation pattern. The angular difference between the highest and minimum angles at which the -3dB beamwidth point occurs is used to calculate the beamwidth for each cut. This calculation method is specified in (2).

$$\theta_{-3dB}^b = |\Theta_{-3dB,2}^b - \Theta_{-3dB,1}^b|, \quad (2)$$

where  $\Theta_{-3dB,1}$ ,  $\Theta_{-3dB,2}$  are the angles at which the radiated power drops to half.

2) *Side Lobe Levels*: The SLL, which is measured in decibels (dB), is the ratio of the side lobes' maximum amplitude to the main lobe's maximum amplitude. as shown in (3):

$$\text{SLL}^b(\text{dB}) = 20 \log_{10} \left( \frac{\text{AP}_{\text{SL,max}}^b}{\text{AP}_{\text{max}}^b} \right), \quad (3)$$

The SLL might not always be in a principal cut throughout this optimization process, which entails turning on and off antenna elements. Instead, it could show up at any arbitrary angular point. In order to determine the overall SLL, the optimizer will look at the complete radiation pattern and find the second-highest maximum, omitting those that are outside the field of view.

### III. ARRAY THINNING ALGORITHM

In large array structures with hundreds of antennas, array thinning is usually done by turning off a certain number of antenna elements depending on the desired SLL. The main benefit of multi-beam array thinning is its contribution to the optimization process in terms of SLL and beamwidth. Since the number of antenna elements is quite large additional flexibility and degrees of freedom can be achieved for the desired results. Therefore, the proposed algorithm first takes into account the desired  $\theta_{-3dB}$ , and SLL.

The minimization problem for the calculated beamwidth ( $\theta_{-3dB_c}(W_{m \times n})$ ), and minimum Side Lobe Level ( $\text{SLL}_c(W_{m \times n})$ ) with the desired counterparts ( $\theta_{-3dB_{Azo}}$ , ( $\text{SLL}_o(W_{m \times n})$ ), respectively, can be defined as:

$$\min_{W_{m \times n}} Z_1(W_{m \times n}) + Z_2(W_{m \times n}) \quad (4)$$

where:

$$\begin{cases} Z_1 = \sum_{r=1}^R \left( \frac{|\theta_{-3dB_r}(W_{m \times n}) - \theta_{-3dB_o}|}{\theta_{-3dB_o}} \right) k_1 \\ Z_2 = \begin{cases} 0, & \text{if } \text{SLL}_c(W_{m \times n}) > 16 \\ \frac{|\text{SLL}_c(W_{m \times n}) - \text{SLL}_o|}{\text{SLL}_o} & \text{if } \text{SLL}_c(W_{m \times n}) \leq 16, \end{cases} \end{cases}$$

and  $k_1$  and  $k_2$  are weights that determine the relative importance of achieving the desired beamwidth versus the side lobe level,  $m$  and  $n$  are the number of antenna elements in  $x$ -axis and  $y$ -axis, respectively, and  $R$  is the number of cuts where the beamwidth will be assessed. The goal of the proposed algorithm is to compute the weight vector, which is crucial for achieving the desired beamwidth and SLL. The weights represent the amplitude and phase of each antenna element. The weight of the  $mn$ -th antenna element,  $W_{m \times n}$ , in a planar array can be calculated as:

$$W_{mnp} = |W_{mnp}| e^{-j\kappa(\sin \theta_0(m d_x \cos \phi_0 + n d_y \sin \phi_0) + p d_z \cos \theta_0)}, \quad (5)$$

where  $(\theta_0, \phi_0)$  represent the scanning angles.

The possibility of an optimization procedure that, particularly when synthesizing beams with various constraints, identifies appropriate configurations to balance antenna element activation. Therefore, in multi-beam scenarios, the number of activation instances of each antenna element can be taken into account as an optimization parameter.

By adopting evenly distributed activation throughout the array, this method improves the system's efficiency as well as overall performance. In addition, by optimizing heat management and power distribution, the sustainability and reliability of the system can be increased.

As a result of controlling activation instances, overall power consumption can be limited by introducing a total power constraint to the system while maintaining the desired beamwidth.

The optimization problem for the multi-beam scenario can be mathematically represented as:

$$\begin{aligned}
& \min_{W^b} f(\theta_{-3dB}^b(W^b), SLL^b(W^b)) \\
& \text{subject to} \quad \sum_{b=1}^B \sum_{m=1}^M \sum_{n=1}^N |W_{m,n}^b|^2 \leq p_{\max} \\
& \quad \sum_{b=1}^B |W^b| \odot |W^b| \leq P_{\max},
\end{aligned} \tag{6}$$

where  $f$  is the cost function and it is defined by (7):

$$\begin{aligned}
f(\theta_{-3dB}^b, SLL^b) &= Z_1(W^b) + Z_2(W^b) \\
Z_1(W^b) &= \frac{1}{B} \sum_{b=1}^B \frac{1}{R} \sum_{r=1}^R \frac{|\theta_{-3dB_r}^b(W^b) - \theta_{-3dB_0}^b(W^b)|}{\theta_{-3dB_0}^b(W^b)} \\
Z_2(W^b) &= \begin{cases} 0, & \text{if } SLL_c^b > 16 \\ \frac{1}{B} \sum_{b=1}^B \frac{|SLL_c^b(W^b) - SLL_0|}{SLL_0}, & \text{if } SLL_c^b \leq 16 \end{cases}
\end{aligned} \tag{7}$$

where  $\theta_{-3dB_0}^b$  is the desired -3 dB beamwidth per beam,  $\theta_{-3dB_c}^b$  is the calculated -3 dB beamwidth per beam,  $SLL_0^b$  is the overall desired SLL per beam,  $SLL_c^b$  is the calculated Side Lobe level per beam,  $W^b$  is the calculated weight matrix per beam,  $p_{\max}$  is the maximum power of the array, and  $P_{\max}$  is the maximum activation times per element matrix.

As a final remark, the proposed multi-beam scenario involves the superimpose of beam power layers which are created concurrently. When operating at the same frequency, superimposing phases require spatial separation to prevent beam distortion. In order to eliminate such a problem, the graph coloring is adopted where each beam is generated by using separate frequency sub-bands. Consequently, the intended beam qualities are preserved by preventing interference.

Following a genetic type of optimization, we derived Algorithm 1 [3] to find the suitable weight matrices that satisfy the problem presented in (6).

The steps of the proposed genetic-based beamforming algorithm are described below:

- **Step 1:** Random initial solution is generated in a tensor where its dimensions are  $M \times B \times N \times C$ ,  $N$ , where  $M$  is the number of rows,  $N$  the number of columns,  $B$  the number of beams, and  $C$  the total number of chromosomes (referred as initial population  $W_o^b$ ).
- **Step 2:** Divide the tensor in dimensions of  $M \times b$ ,  $N$ ,  $C$ , where  $b$  is the beam number.
- **Step 3:** Sort matrices from the lowest to the highest calculated cost values.
- **Step 4:** Eliminate the less efficient half of the stack in Step 3.
- **Step 5:** Repeat the procedure until the threshold. The evolutionary optimization balances the beamwidth and SLL parameters.

---

**Algorithm 1:** Beamforming Algorithm.

---

**Input:**  $(\Lambda^b, \Phi^b)$ , center of the beam in Latitude and longitude coordinates per beam,  
 $\theta_{-3dB_c}^b$ , required beamwidth per beam,  
 $p_{\max}$ , maximum power consumption,  
 $P_{\max}$ , Maximum activation times matrix,  
 $SLL_0^b$ , minimum SLL per beam,

**Output:**  $W^b$ , Weight matrix based on previous inputs

**Data:** Set of possible configurations on Satellite considering system constraints

**Ensure:**  $\sum_{b=1}^B |W^b| \odot |W^b| \leq P_{\max}$

**Ensure:**  $\sum_{b=1}^B \sum_{m=1}^M \sum_{n=1}^N |W_{m,n}^b|^2 \leq p_{\max}$

```

1: Initiate: Population( $W_o^b$ )
2: while Termination criteria not met do
3:   Calculate: Antenna Pattern  $F(W_c^b)$ 
4:   Extract:  $\theta_{-3dB_c}^b$ ,  $SLL_c^b$ ,  $p_{\max}$  and  $P_{\max}$ 
5:   Calculate:  $f(Z_1(W_c^b) + Z_2(W_c^b))$ 
6:   if  $f < f_{\min}$  then
7:     Save: Optimal matrix  $W^b = W_c^b$ 
8:     break
9:   else
10:    Select: Chromosomes based on fitness
11:    Operations: CrossOver and Mutation
12:    Create: New Generation  $W_c^b$ 
13:  end if
14: end while

```

---

#### IV. SIMULATION RESULTS

Given the general characteristics of our evaluation setup, we have analyzed the efficiency of the proposed algorithm under three different scenarios in terms of activation instances. The common parameters for all of the scenarios are given below:

- **Operating Frequency:** 28 GHz.
- **Antenna Array:** 16 x 16 lattice planar array.
- **Orbital Altitude of the satellite:** The orbit of the satellite is considered 500 km above the surface of Earth.
- **Available total power:** We consider 40 dBm total power.
- **SLL:** The SLL is set to 16 dB for each of the synthesized beams.
- **Desired beam widths:** The directions of the desired beams widths in terms of elevation in degrees are given as  $[4.7^\circ, 5.5^\circ, 6^\circ, 6.5^\circ, 5.8^\circ, 5^\circ, 7^\circ]$ .

##### A. Scenario #1

In Scenario #1, the beam synthesis process is subject to specific requirements, as outlined below:

- **Activation instances:** A limit of a maximum of 5 activation instances is imposed on each antenna element.

Detailed results from the beam synthesis Scenario #1 are presented in TABLE I. The activation instances for each antenna element in Scenario #1 is depicted in Fig. 1

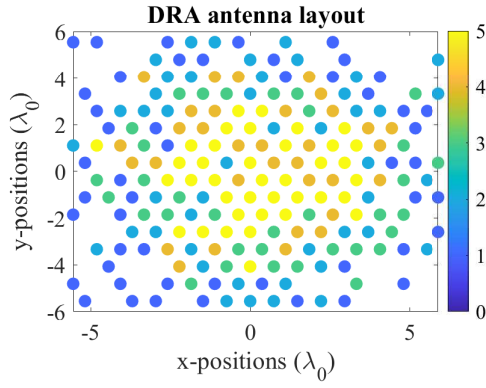


Fig. 1: Activation instances in the DRA for the Scenario #1.

TABLE I: Characteristics of Synthesized Beams in the Scenario #1.

Beam	$\theta_{-3dB_o}$ (°)	$\theta_{-3dB_c}$ (°)	error (%)	SLL (dB)	Act. Elem.	Directivity (dBi)
1	4.7	4.6827	0.3679	15.9	100	27.251
2	5.5	5.4812	0.3418	15.122	78	26.105
3	6	6.0658	1.0975	16.436	77	26.388
4	6.5	6.4505	0.7618	16.056	73	26.091
5	5.8	5.8337	0.581	16.766	86	26.785
6	5	4.9132	1.7363	14.51	87	26.548
7	7	7.0224	0.3196	14.422	65	25.624

### B. Scenario #2

In Scenario #2, the beam synthesis process is subject to specific requirements, as outlined below:

- **Activation instances:** A limit of a maximum of 6 activation instances is imposed on each antenna element.

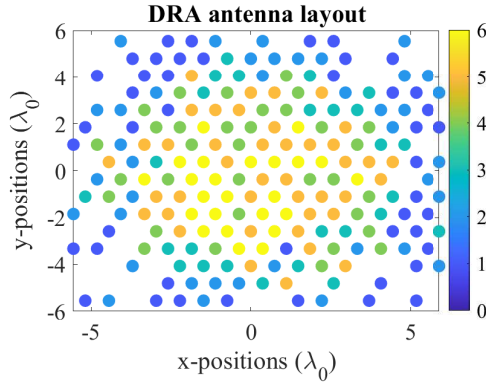


Fig. 2: Activation instances in the DRA for the Scenario #2.

Detailed results from the beam synthesis Scenario #2 are presented in TABLE II. The activation instances for each antenna element in Scenario #2 is depicted in Fig. 2

### C. Scenario #3

In Scenario #3, the beam synthesis process is subject to specific requirements, as outlined below:

TABLE II: Characteristics of Synthesized Beams in the Scenario #2.

Beam	$\theta_{-3dB_o}$ (°)	$\theta_{-3dB_c}$ (°)	error (%)	SLL (dB)	Act. Elem.	Directivity (dBi)
1	4.7	4.7031	0.0663	16.813	118	28.166
2	5.5	5.5041	0.0744	16.56	100	27.383
3	6	6.0245	0.4088	16.249	87	26.853
4	6.5	6.4523	0.7338	17.095	93	27.364
5	5.8	5.814	0.2413	16.766	95	27.366
6	5	4.9863	0.2747	14.51	116	28.109
7	7	7.0353	0.5042	14.422	73	26.283

- **Activation instances:** There is no limit in activation instances, which means that the algorithm will not control the activation but will control the achievement of the SLL and beamwidth.

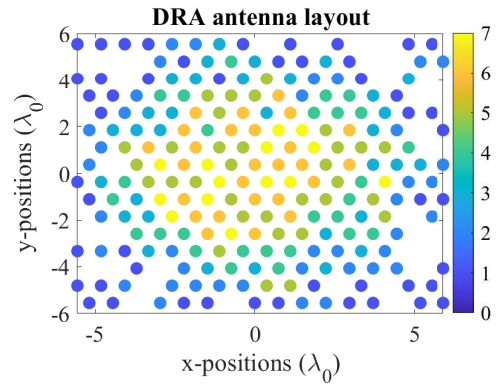


Fig. 3: Activation instances in the DRA for the Scenario #3.

Detailed results from the beam synthesis Scenario #3 are presented in TABLE III. The activation instances for each antenna element in Scenario #3 is depicted in Fig. 3

TABLE III: Characteristics of Synthesized Beams in the Scenario #3.

Beam	$\theta_{-3dB_o}$ (°)	$\theta_{-3dB_c}$ (°)	error (%)	SLL (dB)	Act. Elem.	Directivity (dBi)
1	4.7	4.7003	0.0055	16.86	133	28.826
2	5.5	5.4982	0.0322	17.259	111	27.979
3	6	6.0066	0.1096	16.824	102	27.824
4	6.5	6.4609	0.601	17.095	94	27.58
5	5.8	5.8089	0.1534	16.766	104	27.837
6	5	5.0025	0.0493	16.857	122	28.399
7	7	7.0434	0.6205	16.996	79	26.656

### D. Results Discussion

According to results from each analyzed scenario, as the TABLES I, II and III depicts, the beamwidth variation and error fluctuation decreases as the number of the constrain of maximum activation instances increases. This pattern can be attributed to the number of elements used for each beam,

which limits the precision of beamwidth in all scenarios. The array pattern is calculated using the array multiplication method, which is a numerical method and is simply the product of the array factor and the radiation pattern of the unit cell in a particular direction [3].

On the other hand, it is observed that desired SLL can not be achieved for all the beams in Scenario #1 and Scenario #2, where the activation instances are 5 and 6, respectively, for each antenna element. Since the number of elements required to form a beam reduces as the beamwidth grows there is a correlation between beamwidth and the number of activation instances. It should be noted that that tendency is more obvious in cases where the beamwidth approaches its lower limit. In contrast, in Scenario #3, where the activation sample limit is not considered, it can be seen that all SLL values are below the desired level, regardless of the beamwidth. For a better inspection, the radiation patterns of the beams with the narrowest and widest beamwidths in scenarios Scenario #1, #2, and #3 are given in 4 in the broadside direction.

As a final remark, TABLE IV refers that the sum of the activated elements are almost the same, however, as the number of activation instances increases the overall directivity for each beam increases regardless of the beamwidth and the SLL. Moreover, Equivalent Isotropic Radiated Power (EIRP) per beam can be calculated as:

$$EIRP^b = G^b(\theta, \phi)(dB) + T_x(dBW), \quad (8)$$

where  $G(\theta, \phi)$  is the gain of the optimized antenna in particular direction and  $T_x$  is the transmitted power of the array.

TABLE IV: Number of activation vs. Activated elements for Scenario #1, Scenario #2, and Scenario #3.

Number of Activation	Scenario #1 Act. Ele.	Scenario #2 Act. Ele.	Scenario #3 Act. Ele.
1	46	41	45
2	45	38	34
3	34	26	31
4	33	33	24
5	38	41	37
6	0	24	25
7	0	0	14

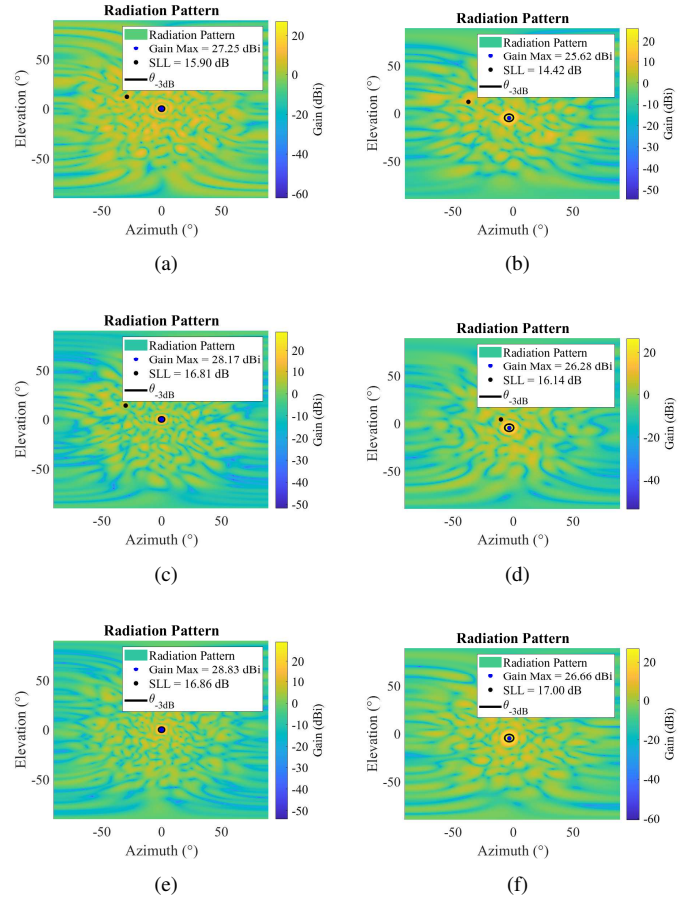


Fig. 4: Radiation patterns in broadside of, a) Beam #1, Scenario #1, b) Beam #7, Scenario #1, c) Beam #1, Scenario #2, d) Beam #7, Scenario #2, e) Beam #1, Scenario #3, and f) Beam #7, Scenario #3.

## V. CONCLUSION

This study presents an approach for synthesizing beam patterns in multi-beam scenarios using a genetic algorithm. The algorithm takes into account parameters such as beamwidth, SLL, element activation instances, and available power. Simulations and results demonstrate the capability of the proposed algorithm to distribute activation instances uniformly across multiple beams and generate effective beamforming. The proposed algorithm is able to prevent saturation in central antenna elements that are more prone to activation in multi-beam scenarios.

Although the results are promising, this study can be extended by application to sector activation antenna instances, effective isotropic radiated power control, null steering (by applying one of the side-lobe cancellation techniques), and regular arrays. Such future research could improve the adaptability and efficiency of beamforming technology in a variety of communication contexts.

## REFERENCES

- [1] E. Brookner, "Phased array radars-past, present and future," in *IEE conference publication*. IET, 2002, pp. 104–113.

- [2] J. S. Herd and M. D. Conway, "The evolution to modern phased array architectures," *Proceedings of the IEEE*, vol. 104, no. 3, pp. 519–529, 2015.
- [3] J. A. Vázquez-Peralvo, J. Querol, F. Ortíz, J. L. González-Rios, E. Lagunas, L. M. Garcés-Socorrás, J. C. M. Duncan, M. O. Mendonça, and S. Chatzinotas, "Multibeam beamforming for direct radiating arrays in satellite communications using genetic algorithm," *IEEE Open Journal of the Communications Society*, 2024.
- [4] R. Palisetty, L. M. G. Socarras, H. Chaker, V. Singh, G. Eappen, W. A. Martins, V. N. Ha, J. A. Vázquez-Peralvo, J. L. G. Rios, J. C. M. Duncan *et al.*, "FPGA implementation of efficient beamformer for on-board processing in meo satellites," in *2023 IEEE 34th Annual International Symposium on Personal, Indoor and Mobile Radio Communications (PIMRC)*. IEEE, 2023, pp. 1–7.
- [5] F. Ortiz, J. A. Vázquez-Peralvo, J. Querol, E. Lagunas, J. L. G. Rios, L. Garcés, V. Monzon-Baeza, and S. Chatzinotas, "Harnessing supervised learning for adaptive beamforming in multibeam satellite systems," in *2024 IEEE International Conference on Machine Learning for Communication and Networking (ICMLCN)*. IEEE, 2024, pp. 386–392.
- [6] R. J. Mailloux, *Phased Array Antenna Handbook*, 3rd ed. Norwood, MA: Artech House, 2018.
- [7] J. A. Vázquez-Peralvo, J. Querol, F. Ortíz, J. L. G. Rios, E. Lagunas, V. M. Baeza, G. Fontanesi, L. M. Garcés-Socorrás, J. C. M. Duncan, and S. Chatzinotas, "Flexible beamforming for direct radiating arrays in satellite communications," *IEEE Access*, 2023.
- [8] G. Fontanesi, F. Ortíz, E. Lagunas, V. M. Baeza, M. Vázquez, J. Vázquez-Peralvo, M. Minardi, H. Vu, P. J. Honnaiah, C. Lacoste *et al.*, "Artificial intelligence for satellite communication and non-terrestrial networks: A survey," *arXiv preprint arXiv:2304.13008*, 2023.
- [9] J. A. Vázquez-Peralvo, J. M. Fernández-González, J. M. Rigelsford, and P. Valtr, "Interwoven hexagonal frequency selective surface: An application for wifi propagation control," *IEEE Access*, vol. 9, pp. 111 552–111 566, 2021.



This figure "EuCAP.png" is available in "png" format from:

<http://arxiv.org/ps/2502.16592v1>



This figure "EurAAP.png" is available in "png" format from:

<http://arxiv.org/ps/2502.16592v1>